
This item was submitted to [Loughborough's Research Repository](#) by the author.
Items in Figshare are protected by copyright, with all rights reserved, unless otherwise indicated.

Evaluation of steel fiber-reinforced sprayed concrete by energy absorption tests

PLEASE CITE THE PUBLISHED VERSION

[https://doi.org/10.1061/\(ASCE\)MT.1943-5533.0003865](https://doi.org/10.1061/(ASCE)MT.1943-5533.0003865)

PUBLISHER

American Society of Civil Engineers

VERSION

AM (Accepted Manuscript)

PUBLISHER STATEMENT

This material may be downloaded for personal use only. Any other use requires prior permission of the American Society of Civil Engineers. This material may be found at [https://doi.org/10.1061/\(ASCE\)MT.1943-5533.0003865](https://doi.org/10.1061/(ASCE)MT.1943-5533.0003865).

LICENCE

All Rights Reserved

REPOSITORY RECORD

Estrada Cáceres, Alan Renato, Sergio Pialarissi-Cavalaro, and Antonio Domingues de Figueiredo. 2021. "Evaluation of Steel Fiber-reinforced Sprayed Concrete by Energy Absorption Tests". Loughborough University. <https://hdl.handle.net/2134/15170253.v1>.

Evaluation of steel fibre reinforced sprayed concrete by energy absorption tests

Alan Renato Estrada Cáceres^{1*}, Sergio Henrique Pialarissi Cavalaro², Antonio Domingues de Figueiredo³,

1. *Dept. of Civil Construction Engineering, Polytechnic School, University of São Paulo, Caixa Postal 61548. CEP 05508-900, Sao Paulo, Brazil, alan.estrada@usp.br.*

2. *School of Architecture, Building and Civil Engineering, Loughborough University, Loughborough, Leics, LE113TU, UK, S.Cavalaro@lboro.ac.uk.*

3. *Dept. of Civil Construction Engineering, Polytechnic School, University of São Paulo, Caixa Postal 61548. CEP 05508-900, Sao Paulo, Brazil, antonio.figueiredo@usp.br.*

* Corresponding author. Tel.: +55 (11) 3091-5165; fax: +55 (11) 3091-5544;
E-mail: alan.estrada@usp.br

Abstract

Steel fibre reinforced sprayed concrete (SFRSC) is widely used for ground support in underground works. The panel test, as in EN 14488-5, is one of the most common procedures for the quality control of the energy absorption capacity of SFRSC. The test entails the deployment of large equipment to manipulate and characterise heavy specimens that cannot be easily extracted from the structure in case a direct assessment of the material in place is needed. Alternative procedures such as the Barcelona test (BCN) have been used to assess the energy absorption of cast fibre-reinforced concrete in smaller-scale cylindrical specimens that can be extracted from the structure and are considerably less demanding in terms of equipment and payload. The objective of this study is to evaluate the use of the BCN in substitution of the traditional square panel test to assess the energy absorption of SFRSC. Both tests were conducted in parallel in combination with the quantification of the incorporated fibre content through the inductive test. Hence, the analysis reflects the actual control conditions of the SFRSC under the influence of the spraying process. Results indicate a possible reliable correlation between the BCN and panel test if the cracked area is considered. Different sizes of cores were tested to understand the influence of this parameter in the energy absorption by the BCN test. The reduction of specimen size demands an increase in the number of determinations per batch to ensure representative results. The study suggests that the BCN can be considered a viable method to evaluate the energy absorption of SFRSC in cores extracted from test panels or actual tunnel linings.

Keywords: *Steel fibre, sprayed concrete, Barcelona test (BCN), square panel test, inductive test, energy absorption.*

1. Introduction

Steel fibres are used in sprayed concrete to provide post-cracking reinforcement to enhance toughness avoiding the typical brittle behavior of this material (Bernard and Thomas 2020) and enhancing dynamic mechanical properties (Chen *et al.* 2020). Steel fibre reinforced sprayed concrete (SFRSC) is widely used in a variety of applications including, construction of slope stabilization, excavation support, structure recovery, refractory lining, tunnel lining, mining operations, etc. (Pfeuffer and Kusterle 2001; Cengiz and Turanli 2004; Bernard 2008; Ginouse and Jolin 2015; Galobardes *et al.* 2019; Liu *et al.* 2020). One of the most traditional applications of SFRSC is tunnel lining by the New Austrian Tunneling Method (NATM). Specifications (e.g. EFNARC 1996, EN 14487-1 2005) classify the SFRSC in this application according to the material energy absorption capacity measured in flexural tests of square panels. The results obtained in the test are used both in the design and systematic quality control. For instance, the Australian Institute of Concrete (2010) takes the energy absorption class measured in the square panel test and the rock formation as input parameters for the tunnel lining design.

The square panel test is currently defined by the standard EN 14488-5 (2006). Modifications in the specimen shape and test procedure proposed to facilitate execution and improve the results include the three-point bending test of square panels with a notch (EFNARC 2011) and round panel test (ASTM C 1550-12 2012). Previous studies have addressed the correlation between different panel shapes (Bernard 2002; Myren and Bjøntegaard 2010) and proposed the use of even larger round panels for increased reliability (Bernard 2013). These methods, however, entail a significant degree of complexity and imply the use of sizeable testing equipment and specimens challenging to produce and manipulate. Possibly the main drawback of these tests lays in the impossibility to extract flat specimens from the curved lining in case a direct verification is needed. Differences in the boundary conditions during the execution of the structure and the panel can lead to different material consolidation and fibre rebound that could compromise the representativeness of the test results (Figueiredo and Helene 1993; Austin *et al.* 1997; Jolin 1999; Armelin and Banthia 2002; Kaufmann *et al.* 2013).

Figueiredo (1997), Bernard (2002), Myren and Bjøntegaard (2010) highlight a significant variability in the panel test results. Papworth (2002) suggests that the non-uniform moulding procedure of panels can lead to inconsistencies in the test results. The production of sufficiently flat, regular specimens is one of the major challenges towards ensuring adequate contact with the support during the test, which might have a significant influence on the results (Bernard 2002). Visual observations reveal that frictional forces between the panel and the supports have a direct impact on the energy absorbed (Myren and Bjøntegaard 2010).

Alternative procedures, such as the Barcelona test (BCN) defined in UNE 83515 (2010), have been used to assess the energy absorption in smaller-scale cast fibre-reinforced concrete (FRC) cylindrical specimens, that can be extracted from the structure and are considerably less demanding in terms of equipment and payload. In the BCN, cylinder punches concentrically placed above and below the specimen produce internal tensile stresses that induce the crack

75 formation and opening. The UNE 83515 (2010) specifies that the increment in specimen
76 perimeter due to cracking should be measured with a circumferential extensometer.

77 Pujadas *et al.* (2013) demonstrate that the increment in perimeter can be calculated from the
78 vertical displacement of the press, thus avoiding the use of the expensive circumferential
79 extensometer not found in most quality control laboratories (Monte *et al.* 2014). The use of this
80 simplified BCN has proved to be an adequate method for the FRC quality control (Simão *et al.*
81 2019). Its application for the assessment of the energy absorption of sprayed FRC and the potential
82 correlation of the results with those obtained through traditional panel tests still lack further
83 research.

84 Carmona *et al.* (2020) correlated the absorbed energy of macro-synthetic fibre reinforced sprayed
85 concrete by means of the BCN test, using a circumferential extensometer, and the square panel
86 test, obtaining good correlation of results. However, the correlation equations were obtained using
87 cast concrete, which differs from sprayed concrete due to the spraying conditions. It was proved
88 by Banthia *et al.* (1994) and Leung *et al.* (2005) that there is no perfect parallelism between the
89 mechanical properties of cast and sprayed FRC in the same dosage.

90 In order to know the actual fibre content incorporated in the structure, a new methodology was
91 developed, the inductive test (Torrents *et al.* 2012; Cavalaro *et al.* 2015). This test can be applied
92 to cylindrical cores (Cavalaro *et al.* 2016) and has been previously used to quantify the fibre
93 content in SFRSC cores (Silva *et al.* 2015; Galobardes *et al.* 2019). Still few studies have been
94 developed considering this method in the evaluation of SFRSC.

95 The objective of this study is to clarify these issues and to evaluate the potential use and
96 implications of the simplified BCN together with the inductive test in substitution of the traditional
97 square panel test. The analysis reflects the real control conditions of the material under the
98 influence of the spraying process. The energy absorption results of two sizes of cylinders tested
99 through the BCN test were correlated with those obtained from the square panel test. Findings
100 derived from this study might support alternative approaches for the quality control of sprayed
101 FRC and enable more straightforward verification of both properties of already built linings and
102 the spraying process conditions.

103

104 **2. Methodology**

105

106 **2.1 Spraying process**

107

108 The mix composition of the concrete is shown in Table 1. The dry materials chosen for the
109 experimental program are commonly used in tunnel linings production in the region of Sao Paulo,
110 Brazil. A polyfunctional admixture based on lignosulphonate solution, a superplasticiser based on
111 a polycarboxilate solution and a hydration stabiliser composed by a sucrose derivate were added
112 to the composition to ensure adequate fresh state properties. The concrete was supplied in a
113 concrete mixer truck.

114 The steel fibre used as reinforcement was classified as type C-II according to the Brazilian standard
115 ABNT NBR 15530: 2007 (2007), with 39 mm length with and aspect ratio of 25 (Figure 1a). This
116 fibre with low aspect-ratio was selected in order to evaluate one of the most critical conditions of
117 SFRSC. Fibres were added in 3 nominal contents (approximately 30, 60 and 90 kg/m³) directly to
118 the truck and mixed thoroughly before the concrete was placed in the pump CP 10-SU (Figure 1b).
119 This equipment has a nominal capacity of spraying of 10 cubic meters per hour and is mainly
120 applied in tunnel linings with cross-sectional area bigger than 40 m². The mixture was sprayed on
121 wood moulds positioned at 20° to the vertical axis (Figure 1c). An accelerator admixture based on
122 aluminium sulphate solution (approximately 24 kg/m³) was used to ensure adequate material
123 consolidation over the surface. The wet spraying process replicates that typically found in ground
124 support applications.

125 Once the production of a test panel series related to lower fibre content was completed, the volume
126 of the remaining concrete was estimated and an extra amount of fibre was added to the concrete
127 truck to achieve the intermediate fibre content. Once the intermediate fibre content test panels were
128 cast, the remaining volume of concrete was again estimated and a last portion of fibres was added
129 to the mix to produce the last series of test panels with the highest fibre content. Notice that
130 ensuring the exact fibre contents of 30, 60 and 90 kg/m³ is not essential for conducting this study
131 as the actual average content was assessed in all cylindrical cores. These nominal fibre contents
132 were chosen aiming to cover the three levels of energy absorption (500, 700, 1000 J) considered
133 in the EN 14487-1 standard, according to the methodology of Figueiredo (1997). The average
134 sprayed concrete compressive strength for each nominal fibre content at 5 months was: 39.1, 38.5
135 and 37.2 MPa, respectively. The results meet the compressive strength requirements for permanent
136 sprayed concrete (30 MPa or greater) (Thomas 2020).

137 The sprayed specimens were square pyramidal truncated panels of two sizes: small panels of 600
138 mm × 600 mm at the base, 800 mm × 800 mm at the top, and thickness of 100 mm; and large
139 panels of 600 mm × 600 mm at the base, 1000 mm × 1000 mm at the top, and thickness 200 mm.
140 4 small panels and 1 large panel were sprayed with each nominal fibre content. An additional small
141 panel was produced for the nominal contents of 60 kg/m³ and 90 kg/m³.

143 **2.2 Square panel test – EN 14488-5**

144
145 At the age of 5 months since production, 14 small panels (4 for the concrete with the lowest
146 nominal fibre content and 5 for each of the others) were tested according to the EN 14488-5 using
147 a 200 tf Shimadzu machine, as shown in Figure 2. A square metal plate (100×100×5 mm) was cast
148 with mortar at the central part of the panels to mitigate irregularities in the spraying surface and
149 ensure uniform load application. The surface of the panel in contact with the mould was positioned
150 on a square steel support, leaving a free square area in the central part of 500 mm side. In some
151 cases, steel thin sheets had to be placed on the edges to obtain a continuous contact between the
152 test panels and the support. The tests were performed at a constant rate of 1 ± 0.1 mm/min. LVDTs
153 were used to measure the displacement, positioned at a yoke fixed at the frame, in order to reduce
154 external deformations. An analysis of the absorbed energy in Joules was made by calculating the
155 area under the load-displacement curve obtained in the tests.

156 2.3 Extraction of cores

157

158 Cylindrical cores were extracted from the panels using a diamond crown cup saw. Large cylinders
159 of nominal size of $\text{Ø}150 \text{ mm} \times 150 \text{ mm}$ (diameter \times height) were extracted from large panels
160 (Figure 3a). Small cylinders of $\text{Ø}100 \text{ mm} \times 100 \text{ mm}$ were extracted from small panels after the
161 flexural test (Figure 3b). This process was performed carefully, avoiding extracting cylinders from
162 cracked regions. The rough end of the core was cut to ensure the same height across all specimens.
163 The specimens were used in the tests described in the next items.

164

165 2.4 Barcelona test

166

167 The test was performed on a 200 tf Shimadzu universal machine following the procedure proposed
168 by Pujadas *et al.* (2013). 18 large cylinders ($\text{Ø}150 \text{ mm} \times 150 \text{ mm}$) and 83 small ones ($\text{Ø}100 \text{ mm}$
169 $\times 100 \text{ mm}$) were tested at 5 and 7 months since production, respectively. The large cylinders are
170 divided in 6 per panel from each fibre content; the small cylinders are divided in 23 from the concrete
171 with lower fibre content (6 per panel minus 1 cylinder that was discarded), 30 from the concrete
172 with the intermediate and higher fibre content, respectively (6 per panel). A constant piston
173 displacement rate of $0.5 \pm 0.05 \text{ mm/min}$ was used in all cases. The cylinders were kept in the same
174 position, that is, the face in contact with the mould at the base of the test machine. The punching
175 load was applied using $\text{Ø}25 \text{ mm} \times 20 \text{ mm}$ steel cylinders for the small specimens and $\text{Ø}37.5 \text{ mm}$
176 $\times 30 \text{ mm}$ for the large ones to comply with the specimen-metallic punch diameter ration of 1/4
177 defined in UNE 83515 (2010). The steel cylinders were concentrically placed on the upper and
178 lower faces of the specimen (Figure 4). The absorbed energy was calculated as the area under the
179 load-displacement curve in Joules.

180

181 2.5 Inductive test

182

183 The fibre content was determined by the inductive test (Torrents *et al.* 2012; Cavalaro *et al.* 2015).
184 Initially, calibration procedure was performed with styrofoam cylinders, three of $\text{Ø}100 \text{ mm} \times 100$
185 mm (785.40 cm^3) and three of $\text{Ø}150 \text{ mm} \times 150 \text{ mm}$ (2650.72 cm^3) in which fibres were inserted
186 manually in a random manner to achieve contents of 30, 60 and 90 kg/m^3 . The inductance change
187 measured can be used to calculate the inductance coefficients for the fibre used, as described in
188 Cavalaro *et al.* (2016). Figure 5 shows the correlations between the fibre content placed in the
189 styrofoam cylinders and the summed inductance variation ΔL_T measured in the 3 orthogonal axes.
190 A linear relationship is both cylinder sizes with intersect 0 (condition without fibre) and a slope β
191 equal to 0.0109 and 0.0103 for large and small cylinders, respectively. The similar β despite the
192 variation on specimens sizes highlights the accuracy of the method.

193 Equation 1 gives the fibre content (C_f) within the cores in kg/m^3 , depending on slop coefficient β ,
194 the total inductance variation (ΔL_T) in mH and volume (V) in m^3 . Since the inductance change
195 produced by concrete and styrofoam is negligible in comparison to that induced by the steel fibres,
196 the same equation and coefficients apply to the cores extracted in the experimental programme.

197

198
$$C_f = \beta \times \frac{\Delta L_T}{V} \quad (1)$$

199

200 The inductive test was performed on the same cylinders used in the BCN test, before undergoing
201 this test. The notations used to present the results are M1, M2 and M3, corresponding to the
202 concretes with nominal fibre contents of 30, 60 and 90 kg/m³, respectively. The letters L and S are
203 added at the beginning of the notation refer to the large and small cylinders, respectively. For
204 example, L_M3 refers to the large cylinders with 90 kg/m³ nominal fibre content.

205

206

207

3. Results and analysis

208

209

3.1 Inductive test

210

211 Table 2 shows the fibre content assessed in the large and small cylinders, including mean values,
212 standard deviation (*SD*), coefficient of variation (*CV*), number of specimens of the sample (*N*),
213 maximum values (*max*) and minimum (*min*). The average fibre content found in specimens L_M1
214 is 46.98 ± 2.19 kg/m³, which is considerably higher than the nominal fibre content of 30 kg/m³.
215 The L_M2 and L_M3 cylinders have similar fibre contents of (79.60 ± 5.96 and 76.85 ± 8.58
216 kg/m³, respectively) despite the difference in the nominal fibre content (60 and 90 kg/m³,
217 respectively).

218

219

220

221

222

223

224

225

Small cylinders S_M1 and S_M2 with the lower and intermediate fibre contents (33.88 ± 4.32 and
63.02 ± 7.31 kg/m³, respectively) show results close to the nominal contents (30 and 60 kg/m³,
respectively), while small cylinders S_M3 with the highest fibre content (74.92 ± 10.24 kg/m³)
display results lower than the nominal value (90 kg/m³). Small cylinders presented a high *CV*
associated to the smaller total weight of fibre within the specimen in comparison with the total
weight found in larger cylinders. This can be intensified by the fact that a fibre with low aspect
ratio was used, which implies a more significant weight variation due to the changes in the number
of fibres in the sample.

226

227

228

229

230

For subsequent analysis, the average fibre content measured for the cylinders, determined by the
inductive test, will be used. The fibre contents obtained in the small cylinders also correspond to
the small panels from which they were extracted, and will be used in the evaluation of the square
panel test EN 14488-5.

231

3.2 Square panel test – EN 14488-5

232

233

234

235

236

237

Figure 6 shows the mean load (*P*) versus displacement (δ) and absorbed energy (*E*) versus
displacement (δ) curves. Table 3 summarises the energy absorption for a displacement of 25 mm
(*E*₂₅), the panel thickness (*h*) and the number of cracks (*N*_{*c*}) after the test, considering the major
and minor cracks. The mean values, standard deviation (*SD*), coefficient of variation (*CV*), sample
size (*N*), and maximum (*max*) and minimum (*min*) values are also provided.

238 Both fibre content and panel thickness influence the energy absorption results in Table 3. The
239 panels with higher fibre content (74.92 kg/m^3) and higher thickness (121.25 mm) show the highest
240 average energy absorption value ($976.18 \pm 174.51 \text{ J}$), followed by the panels with fibre contents
241 of 63.02 and 33.88 kg/m^3 , which have energy absorption values of 578.18 ± 47.22 and $488.85 \pm$
242 50.38 J , respectively. The cracking pattern was generally 4 cross-shaped major cracks in panels
243 with fibre contents of 33.88 and 63.02 kg/m^3 (Figure 7a). The number of cracks tends to increase
244 for the content of 74.92 kg/m^3 . For example, the panel with the highest energy absorption value of
245 1176.07 J presented 5 major and 2 minor cracks (Figure 7b). Panels with lower and medium fibre
246 contents show a smaller number of cracks because a simple biaxial flexion occurs. As fibre content
247 increases, the degree of redundancy in the test increases (Myren and Bjøntegaard 2010; Salehian
248 *et al.* 2014; Juhasz *et al.* 2017); this in addition to the friction forces in the supports cause punching
249 shear failure (Carmona *et al.* 2020), therefore the number of cracks increases. Cracking close to
250 the edge of the panel could be highly affected by the support. Future studies focusing on that matter
251 are needed.

252 The influence of the panel thicknesses on the absorbed energy was also reported by Bjøntegaard
253 (2009), Myren and Bjøntegaard (2010), Sandbakk (2011). A correction factor, based on the study
254 of Thorenfeldt (2009) *apud* Myren and Bjøntegaard (2010) was applied to compensate for this
255 influence. The procedure is as follows: firstly, a corrected displacement must be found ($\Delta = 25$
256 $\text{mm} \times k$, $k = 100/h$); then, the corrected energy (E_C) is the energy corresponding to the corrected
257 displacement (E_Δ) multiplied by the factor k ($E_C = E_\Delta \times k$).

258 From Table 3 the corrected energy absorption results (E_C) are: 397.85 ± 30.31 , 494.18 ± 37.12 ,
259 $758.88 \pm 147.15 \text{ J}$, for the panels with fibre contents of 33.88, 63.02 and 74.92 kg/m^3 , respectively.
260 These results will be used for further analysis in following sections. Similar CVs were found for
261 the two lowest fibre contents. The considerably higher CV observed for specimens with the highest
262 fibre content is probably due to the more pronounced variation in thickness and number of cracks
263 in these panels. Microcracks or internal cracks could also influence differently the CV of tested
264 panels with high and low fibre content. However, the presence of such microcracks was not
265 assessable in the study.

266 267 **3.3 Barcelona test**

268
269 Figure 8 shows the mean load (P) and absorbed energy (E) versus displacement (δ) curves of the
270 cylinders extracted from the panels of each mixture, of the two days of spraying. The curves were
271 considered only from the displacement relative to the peak load reached in the test.

272 The results of energy absorption by displacement of the extracted cylinders are presented in Table
273 4. The results are evaluated up to the post-peak displacement of 5.0 mm, following the same
274 criteria of previous studies that assess the absorbed energy in regular displacements in FRC
275 (Galobardes and Figueiredo 2015; Liu *et al.* 2018) and SFRSC (Silva 2017; Galobardes *et al.*
276 2019) through the BCN test.

277 The load results are not considered in the analysis since they are not part of the study. The mean
278 values, the standard deviation (*SD*), coefficient of variation (*CV*), sample size (*N*), maximum (*max*)
279 and minimum (*min*) values are presented in Table 4.

280 From Table 4 analyzing the energy absorption results of the large cylinders in the displacement of
281 5 mm, the absorbed energies in increasing order are: 79.07 ± 17.61 , 154.67 ± 26.64 , $189.24 \pm$
282 39.81 J, for the cylinders with fibre contents of 46.98, 79.60 and 76.85 kg/m^3 , respectively. It is
283 observed that the cylinders with fibre content of 76.85 kg/m^3 show a higher level of energy
284 absorption in relation to the cylinders of 79.60 kg/m^3 , despite having lower fibre content. This may
285 also be due to a better orientation in relation to the crack surface which may occurs randomly.

286 Analyzing the average absorption results of the small cylinders, the absorbed energies at 5 mm
287 are: 34.18 ± 12.36 , 60.35 ± 16.41 and 69.91 ± 15.04 J, for the cylinders with fibre contents of
288 33.88, 63.02 and 74.92 kg/m^3 , respectively. The increasing order in energy absorption is related to
289 the fibre content. The *CVs* were generally higher for the small cylinders, following the trend
290 observed in the fibre content, as expected and better discussed in the next section.

291

292 **3.4 Comparison of coefficients of variation**

293

294 Figure 9 shows the *CVs* of the energy absorption results obtained from the square panel tests EN
295 14488-5 (Table 3) and BCN tests (Table 4). It can be seen that the higher *CVs* correspond to the
296 small cylinders of the BCN test, with a mean *CV* of 28.29%. In an intermediate situation are the
297 large cylinders of the BCN test, with mean *CV* of 20.18%. The panels have the smallest variation,
298 with a mean *CV* of 11.51%.

299 In general, the *CV* of the absorbed energies is higher for small specimens. The *CVs* obtained with
300 small cylinders were higher than those of the large ones, although they have lower amplitude of
301 results. Similar trend was found by Aire *et al.* (2007), who evaluated the FRC in different sizes of
302 cylinders, using the BCN test. This behavior can also be associated with the size of the specimen
303 that defines the area of the fractured section. The larger this area, the smaller the coefficient of
304 variation as observed in the study by Cavalaro and Aguado (2015). And also, in the small cylinders
305 the *CVs* decrease since the fibre content increase, while in the large remains practically constant
306 in all mixtures. These facts show that the large cylinders maintain a more stable behavior during
307 the BCN test.

308 The *CVs* obtained in the EN 14488-5 panel tests were lower than the *CVs* obtained with the BCN
309 tests for each mixture. This fact may be due to having a larger fracture surface. Similarly, it may
310 be due to the fact that great care was taken before the test, by placing metal plates to ensure a
311 continuous contact between the panels and the support; and during spraying, avoiding buckling on
312 the panels. Several authors report that *CV* decreases with enhancing the fracture surface (Carmona
313 *et al.* 2018). Nonetheless, the *CV* increases in the mixture with higher fibre content. This may be
314 due to the fact that panels of 74.92 kg/m^3 , besides the higher fibre content, have the greatest
315 thickness and number of cracks variation, resulting in a greater variation of energy absorption
316 results.

317

318 **3.5 Mix design correlations and comparative analysis**

319

320 The comparative analysis of the absorbed energy of the SFRSC is based on the analysis of mix
321 design correlations. These correlations are focused on the average energy absorption results,
322 between the square panel tests EN 14488-5 and BCN tests (Tables 3 and 4, respectively). The R^2
323 resulting for the correlations between the square panel test EN 14488-5 and BCN tests on small
324 and large cylinders are almost similar, with values of 0.9809 and 0.9798, respectively (Figure 10).
325 The good correlations indicate that any of the cylinders can be used in the evaluation of the energy
326 absorption of the SFRSC, replacing the panels.

327 The comparative analysis is also based on the correlation of the energy absorption results of the
328 square panel test EN 14488-5 and BCN tests on both size of cylinders with the fibre content, in
329 each evaluated element (individual results that generated Tables 2-4). These correlations are
330 shown in Figure 11a. The best correlation corresponds to the square panel test ($R^2 = 0.9714$), with
331 sample size of 14 panels. The correlations obtained in the BCN tests on small and large cylinders
332 were 0.9538 and 0.9568, with sample sizes of 83 and 18 cylinders, respectively.

333 The experimental design generated the difference in the number of parameters points of the tests
334 in the linear fittings in Figure 11. In the case of the square panel test, the sample type and number
335 respond to those typically adopted for the quality control of shotcrete. Since the BCN is an
336 alternative test without the support of specific standards for shotcrete, the number of specimens
337 was increased to evaluate the significance of the test variability.

338 To further verify the correspondence between the test methods, the absorbed energy results were
339 divided by the crack area of each specimen tested. In the BCN tests, the absorbed energy was
340 divided by the area of the rectangle that forms the cylinder, multiplied by three, since this is the
341 number of cracks that commonly appear in this test (Pujadas 2013). In the panels, the absorbed
342 energy was divided by the cross-sectional area multiplied by two, since the cracking pattern was
343 generally 4 cross-shaped major cracks. The correlations between energy absorbed per area and
344 fibre content are shown in Figure 11b. It can be seen that the three tests have similar trend lines.
345 Grouping into a single correlation, the trend line equation is: $y = 63.584 x$, with an R^2 value of
346 0.9562. This fact reinforces the concept that the tests are correlated with each other. It is also
347 noteworthy that the absorbed energy results have an almost constant range as the fibre content
348 increases.

349 From Figure 11a it is possible to determine which energy level corresponds to each test for a given
350 fibre content. This can be used to evaluate the SFRSC by the BCN test, according to design
351 methods based on square panel tests results, such as the EN 14487-1 (2005) standard.

352 According to the EN 14487-1, in the square panel test, to evaluate the SFRSC, three energy
353 absorption levels are considered, in 25 mm of displacement. This type of classification can be
354 associated with empirical tunnel sizing methods, which define the application of SFRSC according
355 to the competence of the rock mass (Barton 2002; Shotcreting in Australia: Recommended Practice
356 2010; Rehman *et al.* 2019). The energy requirements are: class E 500, E 700, and E 1000 of 500
357 J, 700 J, and 1000 J, respectively. From Figure 11a, the energy absorption levels of the BCN test,

358 on large and small cylinders, that correspond to these energy requirements and the average fibre
359 content to achieve these energies, are shown in Table 5. Because all regressions in Figure 11a are
360 linear, there may be a linear relationship between the values obtained. However, specific studies
361 need to be done to obtain correlations of energy absorption with other types of fibres.

362 The energy requirements for each test and average fibre content were calculated considering the
363 confidence intervals of linear regression, at 90% of confidence level, obtained from individual
364 results that generated Tables 2, 3 and 4, according to the method of Freund and Simon (2002). The
365 confidence intervals are presented in brackets in Table 5 and are also shown with dashed lines in
366 Figure 11a.

367

368 **3.6 Sample size analysis**

369

370 A very common question for tunnel designers and builders is about the representative sample size
371 in order to evaluate a structure. For this, according to the results, the reliable sample size was
372 determined using the method of Bussab and Moretin (2002), through Equation 2, where the
373 statistical values are: the sample size (n); the t-distribution (t) according to the confidence level
374 (α); standard deviation (SD); and the acceptable error. In the present case, it was considered an
375 average value according to the CV s evaluated, i.e. 20% of the mean value (e). Table 6 shows the
376 comparison of sample sizes obtained for BCN tests on small and large cylinders and for the square
377 panel test EN 14488-5, according to the results of Tables 4 and 3, respectively.

$$378 \quad n = \frac{\tau_{n-1}^2 \cdot s^2}{e^2} \quad (2)$$

379 Evaluating sample sizes at 95% of confidence level, for the BCN test on large cylinders, the sample
380 is almost constant for all mixtures, ranging from 5 to 9 cylinders. The BCN test on small cylinders
381 needs a larger sample of 15 cylinders for lower fibre content (33.88 kg/m³). For larger fibre
382 contents (63.02 and 74.92 kg/m³) the sample decreases to 8 and 5 cylinders, respectively. In the
383 case of the square panel test, only 2 samples are required for mixtures of 33.88 and 63.02 kg/m³.
384 However, for the mixture with higher fibre content (74.92 kg/m³), 8 panels are required. The
385 increase in the number of specimens demanded for the EN 14488-5 test with the highest fibre
386 content was due to the increase in CV of this serie, which was generated by the variation of panel
387 thickness and number of cracks. This tendency of increasing number of specimens associate to the
388 highest fibre content was not so evident for the BCN tests that presented higher uniformity on
389 geometry and crack pattern characteristics.

390 This high number of specimens can also be attributed to the fact that the fibre used has a low aspect
391 ratio. As a result, the reinforcement capacity is more susceptible to variations in the number of
392 fibres present in the cracking area. Therefore, this evaluation can be considered as critical and the
393 number of specimens indicated must meet the confidence level for sprayed concretes reinforced
394 with fibre with higher aspect ratio. Considering that the number of specimens in the sample show
395 to be below the desired for a few test conditions, the findings represent a valid contribution to the
396 literature.

397 Although the cylinders for the BCN tests need a larger number of samples, they can easily be
398 handled and transported, as the small cylinder weighs around 2 kg and the large 6.5 kg, much less
399 compared to the small panels for the square panel test, which weighs around 110 kg. This fact
400 would evidently improve the technology control process both on site and in the laboratory, besides
401 the advantage of being able to extract cores directly from the structure in different locations.
402 However, in cases of evaluation of existing structures it may be necessary to extract a larger
403 number of specimens to obtain representative results.

404

405 **4. Conclusions**

406

407 The study showed the possibility of correlation between the results obtained of energy absorption
408 in the BCN tests in small and large extracted cylinders and the square panel test EN 14488-5. The
409 main conclusions were:

- 410 • It was confirmed that the level of energy absorption is directly related to the actual fibre
411 content of the SFRSC, being able to determine which energy level corresponds to each test
412 for a given fibre content. By dividing the energy absorption by the fracture area observed
413 in the specimens of each test they practically maintain the same trend line, showing the
414 correspondency between all tests.
- 415 • The CV of energy absorption associate to the small cylinders is higher than those of the
416 large ones. In the small cylinders the CVs decrease since the fibre content enhance, while
417 in the large remains almost constant. This shows that the large cylinders provide more
418 uniform results from the BCN test due to the larger crack area. The panel tests have the
419 smallest CV which could be associated to the even larger fracture surface. However, the
420 CV increases at higher fibre contents due to variations in the number of the cracks together
421 with the panel's thickness in this particular case. Thus, the production of specimens for this
422 type of test should be careful to minimize the variation of their final thickness.
- 423 • The largest CV of the BCN test is clearly disadvantageous, in order to obtain representative
424 results. Nonetheless, the BCN test can be used for routine control and, especially for
425 existing SFRSC structures evaluation once it becomes possible to perform the test with
426 extracted cores. Also, the BCN test has the advantage of using smaller equipment and the
427 smaller specimens produce much better working conditions for operators in the laboratory.
- 428 • The good correlations of the absorbed energy results of the square panel test and BCN in
429 extracted cylinders, justify the use of any of the cylinders in the evaluation of the absorbed
430 energy of the SFRSC. The BCN test can be considered as representative to evaluate the
431 values of absorbed energy in underground works of SFRSC, as long as the correspondence
432 of absorbed energy is established in previous studies.
- 433 • Cylindrical cores can be extracted *in situ* allowing evaluate the tunnel lining real
434 conditions. The fact that the specimens can be used for two determinations (fibre content
435 effectively incorporated into the structure and determination of the mechanical behavior of
436 the SFRSC) expands the quality control potential of the tunnel lining construction,
437 providing greater reliability in the process. However, the obtained correlations could not

438 be extrapolated and, in consequence they must be determined for each project in the
439 previous qualification studies of the SFRSC.

440 **Data availability**

441
442 All data, models, and code generated or used during the study appear in the submitted article.
443

444 **Acknowledgements**

445
446 The authors gratefully acknowledge for the support of P&D ANEEL (Pesquisa e Desenvolvimento
447 - Agencia Nacional de Energia Eletrica, Brasil) and Brazilian companies: CPB (Concreto
448 Projetado Brasil), Solotrat Engenharia and Holcim Brasil. The first and third author would like to
449 thank the National Council for Scientific and Technological Development (Conselho Nacional de
450 Desenvolvimento Científico e Tecnológico – CNPq, Brasil) for the support provided through the
451 doctoral scholarship and financial resources provide by the research project (Proc. N°:
452 305055/2019-4).

453

5. References

- 456 AENOR (Asociación Española de Normalización y Certificación). (2010). “Hormigones con
457 fibras. Determinación de la resistencia a fisuración, tenacidad y resistencia residual a
458 tracción. Método Barcelona.” *UNE 83515: 2010*, Madrid, Spain. (in Spanish).
- 459 Aire, C., Molins, C., and Aguado, A. (2013). “Ensayo de doble punzonamiento para concreto
460 reforzado con fibra: efecto del tamaño y origen de la probeta.” *Concreto y Cemento.
461 Investigación y Desarrollo*, 5(1), 17-31. (in Spanish).
- 462 ASTM (American Society for Testing Materials). (2012). *Standard test method for flexural
463 toughness of fiber reinforced concrete (using centrally loaded round panel)*, ASTM
464 C1550-12. West Conshohocken, PA: ASTM.
- 465 Armelin, H. S., and Banthia, N. (2002). “A novel double anchored steel fiber for shotcrete.”
466 *Canadian Journal of Civil Engineering*, 29, 58–63.
- 467 ABNT (Associação Brasileira Normas Técnicas). (2007). “Fibras de aço para concreto -
468 especificações.” *ABNT. NBR 15530: 2007*, Rio de Janeiro, Brazil. (in Portuguese).
- 469 Austin, S. A., Peaston, C. H., and Robins, P. J. (1997). “Material and fibre losses with fibre
470 reinforced sprayed concrete.” *Construction and Building Materials*, 11(5-6), 291-298.
- 471 Banthia, N., Trottier, J-F., and Beaupré, D. (1994). “Steel-fiber-reinforced wet mix shotcrete:
472 comparison with cast concrete.” *Journal of Materials in Civil Engineering. American
473 Society of Civil Engineers*, 6(3), 430-437.
- 474 Barton, N. (2002). “Some new Q-value correlations to assist in site characterization and tunnel
475 design.” *International Journal of Rock Mechanics and Mining Sciences*, 39, 185-216,.
- 476 Bjøntegaard, Ø. (2009). “Energy absorption capacity for fibre reinforced sprayed concrete. Effect
477 of friction on round and square panel tests whit continuous support (Series 4).” *Norwegian
478 Public Roads Administration*, Technology report n^o 2534, 1-53.
- 479 Bernard, E. S. (2002). “Correlations in the behaviour of fibre reinforced sprayed concrete beam
480 and panel specimens.” *Materials and Structures*, 35, 156-164.
- 481 Bernard, E. S. (2008). “Early-age load resistance of fibre reinforced shotcrete linings.” *Tunnelling
482 and Underground Space Technology*, 23(4), 451-460.
- 483 Bernard, E. S. (2013). “Development of a 1200-mm-Diameter Round Panel Test for Post-Crack
484 Assessment of Fiber-Reinforced Concrete.” *Advanced in Civil Engineering Materials*,
485 2(1), 457-471.
- 486 Bernard, E. S., and Thomas, A. H. (2020). “Fibre reinforced sprayed concrete for ground support.”
487 *Tunnelling and Underground Space Technology*, 99, 103302.
- 488 Bussab, W., and Moretim, P. (2002). *Estatística básica*, 5ed., Editora Saraiva, São Paulo. (in
489 Portuguese).
- 490 Carmona, S., Molins, C., and Aguado, A. (2018). “Correlation between bending test and Barcelona
491 tests to determine FRC properties.” *Construction and Building Materials*, 181, 673-686.
- 492 Carmona, S., Molins, C., and García, S. (2020). “Application of Barcelona test for controlling
493 energy absorption capacity of FRS in underground mining works.” *Construction and
494 Building Materials*, 246, 118458.
- 495 Cavalaro, S. H. P., and Aguado, A. (2015). “Intrinsic scatter of FRC: an alternative philosophy to
496 estimate characteristic values.” *Materials and Structures*, 48(11), 3537–3555.
- 497 Cavalaro, S. H. P., López, R., Torrents, J. M., and Aguado, A. (2015). “Improved assessment of
498 fibre content and orientation with inductive method in SFRC.” *Materials and Structures*,
499 48(6), 1859-1873.
- 500 Cavalaro, S. H. P., López, R.; Torrents, J. M., Aguado, A., and García, P. (2016). “Assessment of
501 fibre content and 3D profile in cylindrical SFRC specimens.” *Materials and Structures*,
502 49(1-2), 577-595.

503 Cengiz, O., and Turanli, L. (2004). "Comparative evaluation of steel mesh, steel fibre and high-
504 performance polypropylene fibre reinforced shotcrete in panel test." *Cement and Concrete*
505 *Research*, 34(8), 1357-1364.

506 Chen, L., Zhang, X., and Liu, G. (2020). "Analysis of dynamic mechanical properties of sprayed
507 fiber-reinforced concrete based on the energy conversion principle." *Construction and*
508 *Building Materials*, 254, 119167.

509 EFNARC (European Federation of Producers and Applicators of Specialist Products for
510 Structure). (1996). "European Specification for Sprayed Concrete." EFNARC, Hampshire,
511 UK.

512 EFNARC (European Federation of Producers and Applicators of Specialist Products for
513 Structure). (2011). "Testing Sprayed Concrete. EFNARC Three Point Bending Test on
514 Square Panel with Notch". EFNARC, Hampshire, UK.

515 EN 14487-1 (European Standard). (2005). "Sprayed concrete – Part 1: Definitions, specifications
516 and conformity." *EN 14487-1: 2005*, Brussels, Belgium.

517 EN 14488-5 (European Standard). (2006). "Testing sprayed concrete – Part 5: Determination of
518 energy absorption capacity of fibre reinforced slab specimens." *EN 14488-5: 2006*,
519 Brussels, Belgium.

520 Figueiredo, A. D., and Helene, P. R. L. (1993). "Reflexões sobre a reflexão." *Téchne-Revista de*
521 *Tecnologia da Construção*, Ed. PINI Nº 5, 24-27. (in Portuguese).

522 Figueiredo, A. D. (1997). "Parâmetros de controle e dosagem do concreto projetado com fibras de
523 aço". Thesis (Doctorate). Escola Politécnica, University of São Paulo, São Paulo, Brazil.
524 (in Portuguese).

525 Freund, J. E., and Simon, G. A. (2002). *Estatística aplicada. Economia, administração e*
526 *contabilidade*, 9ed., Bookman, Porto Alegre. (in Portuguese).

527 Galobardes, I., and Figueiredo, A. D. (2015). "Correlation between beam and Barcelona tests for
528 FRC quality control for structural application". *Fibre Concrete 2015. September 10-11*,
529 Prague, Czech Republic.

530 Galobardes I., Silva, C. S., Figueiredo, A. D., Cavalaro, S. H. P., and Goodier, C. I. (2019).
531 "Alternative control of steel fibre reinforced sprayed concrete (SFRSC)." *Construction and*
532 *Building Materials*, 223, 1008 – 1015.

533 Ginouse, N., and Jolin, M. (2015). "Investigation of spray pattern in shotcrete applications." *Construction and Building Materials*, 93, 966-972.

534 Jolin, M. (1999). "Mechanisms of placement and stability of dry process shotcrete." Thesis (PhD)
535 – Department of civil engineering, The University of British Columbia, Vancouver,
536 Canada.

537 Juhasz, P. K., Nagy, L., and Schaul, P. (2017). "Correlation of the results of the standard beam
538 and EFNARC panel test". In *Proceedings of the World Tunnel Congress 2017 – Surface*
539 *challenges – Underground Solutions*, Bergen, Norway: International Tunnelling and
540 Underground Space Association.

541 Kaufmann, J., Frech, K., Schuetz, F., and Münch, B. (2013). "Rebound and orientation of fibers
542 in wet sprayed concrete applications." *Construction and Building Materials*, 49, 15-22.

543 Leung, C. K. Y., Lai, R, and Lee, A. Y. F. (2005). "Properties of wet-mixed fiber reinforced
544 shotcrete and fibre reinforced concrete with similar composition." *Cement and Concrete*
545 *Research*, 35(4), 788-795.

546 Liu, X., Yan, M, Galobardes, I., and Sikora, K. (2018). "Assessing the potential of functionally
547 graded concrete using fibre reinforced and recycled aggregate concrete." *Construction and*
548 *Building Materials*, 171, 793-801.

549 Liu, G., Cheng, W., Chen, L., Pan, G., and Liu, Z. (2020). "Rheological properties of fresh concrete
550 and its application on shotcrete." *Construction and Building Materials*, 243, 118180.

551

552 Monte, R., Toaldo, G. S., and Figueiredo, A. D. (2014). “Avaliação da tenacidade de concretos
553 reforçados com fibras através de ensaios com sistema aberto”, *Matéria (Rio Janeiro)*, 19,
554 132–149. (in Portuguese).

555 Myren, S. A., and Bjøntegaard, Ø. (2010). “Round and square panel tests – a comparative study.”
556 *Shotcrete: Elements of a System – Bernard (ed)*. Taylor & Francis Group, London.

557 Papworth, F. (2002). “Design guidelines for the use of fibre reinforced sprayed concrete in ground
558 support”, *27th conference on Our World in Concrete & Structures: August 29-30, 2002*,
559 Singapore: CI-Premier PTE.

560 Pfeuffer, M., and Kusterle, W. (2001). “Rheology and rebound behaviour of dry-mix shotcrete”.
561 *Cement and Concrete Research*, 31(11), 1619-1625.

562 Pujadas, P. (2013). “Caracterización y diseño del hormigón reforzado con fibras plásticas.” Thesis
563 doctoral, Dept. of Civil and Environmental Engineering, Polytecnic Univ. of Catalonia.
564 (in Spanish).

565 Pujadas, P., Blanco, A., Cavalaro, S. H. P., de la Fuente, A. and Aguado, A. (2013). “New
566 analytical model to generalize the Barcelona test using axial displacement.” *Journal of*
567 *Civil Engineering and Management*, 19(2), 259-271.

568 Rehman, H., Naji, A. M., Kim, J-J., and Yoo, H. (2019). “Extension of tunneling quality index
569 and rock mass rating systems for tunnel support design through back calculations in highly
570 stressed jointed rock mass: An empirical approach based on tunneling data from
571 Himalaya.” *Tunnelling and Underground Space Technology*, 85, 29-42.

572 Salehian, H., Barros, J. A. O., and Taheri, M. (2014). “Evaluation of the influence of post-cracking
573 response of steel fibre reinforced concrete (SFRC) on load carrying capacity of SFRC
574 panels.” *Construction and Building Materials*, 73, 289-304.

575 Sandbakk, S. (2011). “Fibre Reinforced Concrete Evaluation of test methods and material
576 development.” Doctoral Thesis, Dept. of Structural Engineering, Norwegian Univ. of
577 Science and Technology.

578 Shotcreting in Australia: Recommended Practice. Second edition. (2010). Concrete Institute of
579 Australia & AuSS, Sydney.

580 Silva, C. L., Galobardes, I., Pujadas, P., Monte, R., Figueiredo, A. D., Cavalaro, S. H. P., and
581 Aguado, A. (2015). “Assessment of Fibre Content and Orientation in SFRC with the
582 Inductive Method. Part 2: Application for the Quality Control of Sprayed Concrete.” *E-*
583 *Journal of Nondestructive Testing and Ultrason-ics*, 20, 18384.

584 Silva, C. L. (2017). “Proposta de metodologia alternativa para controle de qualidade da aplicação
585 estrutural do concreto projetado reforçado com fibras de aço.”. Dissertação (Mestrado).
586 Dept. of Civil Construction Engineering, Universidade de São Paulo. (in Portuguese).

587 Simão, L. C. R., Nogueira, A. B., Monte, R., Salvador, R. P., and Figueiredo, A. D. (2019).
588 “Influence of the instability of the double punch test on the post-crack response of fiber-
589 reinforced concrete.” *Construction and Building Materials*, 217, 185-192.

590 Thomas, A. (2020). *Sprayed Concrete Lined Tunnels*. 2nd ed., Taylor & Francis, London and New
591 York.

592 Thorenfeldt, E. 2006. “Fibre reinforced concrete panels. Energy absorption capacity for standard
593 samples.” SINTEF memo. SINTEF Memo. Oslo, Norway: Norwegian Public Roads
594 Administration. (in Norwegian).

595 Torrents, J. M., Blanco, A., Pujadas, P., Aguado, A.; Juan-García, P., and Sánchez-Moragues, M.
596 A. (2012). “Inductive method for assessing the amount and orientation of steel fibers in
597 concrete.” *Materials and Structures*, 45(10), 1577–1592.

598

Table 1 – Concrete mix composition.

| Materials | Content (kg/m ³) |
|---|---------------------------------|
| Cement (70% CEM I 52.5R and 30% blast-furnace slag) | 400 |
| Fine quartz sand (0 - 0.6 mm) | 574 |
| Crushed granitic sand (0 - 4.8 mm) | 315 |
| Crushed granite coarse aggregate (4.8 - 12.5 mm) | 840 |
| Water | 200 |
| Polyfunctional admixture | 1.44 |
| Superplasticiser | 0.84 |
| Hydration stabilizer | 1.12 |

Table 2: Fibre content (C_f) in kg/m³ of the extracted cylinders.

| | Cylinders of Ø150 mm × 150 mm | | | Cylinders of Ø100 mm × 100 mm | | | |
|---------------|-------------------------------|-------|-------|-------------------------------|-------|-------|-------|
| | L_M1 | L_M2 | L_M3 | S_M1 | S_M2 | S_M3 | |
| Mean | 46.98 | 79.60 | 76.85 | Mean | 33.88 | 63.02 | 74.92 |
| SD | 2.19 | 5.96 | 8.58 | SD | 4.32 | 7.31 | 10.24 |
| CV (%) | 4.67 | 7.48 | 11.16 | CV (%) | 12.75 | 11.60 | 13.66 |
| N | 6 | 6 | 6 | N | 23 | 30 | 30 |
| max | 49.45 | 89.38 | 86.46 | max | 47.05 | 82.27 | 93.48 |
| min | 44.28 | 71.23 | 63.55 | min | 24.66 | 51.80 | 54.02 |

604 **Table 3:** Absorbed energy in 25 mm (E_{25}) in J for smaller panels according to EN 14488-5, panel thickness
605 (h) in mm, number of cracks on the panels (N_c) after being tested, factor of correction (k), modified
606 displacement (Δ) in mm, corrected absorbed energy (E_c) in J.

| | Panels ($C_f = 33.88$ kg/m ³) | | | | | | Panels ($C_f = 63.02$ kg/m ³) | | | | | | |
|---------------|--|--------|-------|------|----------------------|--------------------------|--|--------|--------|-------|----------------------|--------------------------|--------|
| | E_{25} | h | N_c | k | $\Delta =$ $25.k$ | $E_c = K.$ E_Δ | E_{25} | h | N_c | k | $\Delta =$ $25.k$ | $E_c = K.$ E_Δ | |
| Mean | 488.85 | 117.61 | 3.75 | 0.85 | 21.28 | 397.85 | Mean | 578.18 | 112.05 | 4.40 | 0.89 | 22.31 | 494.18 |
| SD | 50.38 | 4.02 | 0.50 | 0.03 | 0.72 | 30.31 | SD | 47.22 | 1.51 | 0.55 | 0.01 | 0.30 | 37.12 |
| CV (%) | 10.31 | 3.42 | 13.33 | 3.37 | 3.37 | 7.62 | CV (%) | 8.17 | 1.35 | 12.45 | 1.34 | 1.34 | 7.51 |
| N | 4 | 4 | 4 | 4 | 4 | 4 | N | 5 | 5 | 5 | 5 | 5 | 5 |
| max | 538.51 | 122.99 | 4.00 | 0.88 | 21.93 | 422.11 | max | 629.05 | 114.29 | 5.00 | 0.90 | 22.57 | 542.63 |
| min | 424.94 | 113.98 | 3.00 | 0.81 | 20.33 | 354.17 | min | 505.37 | 110.77 | 4.00 | 0.87 | 21.87 | 440.22 |

| | Panels ($C_f = 74.92$ kg/m ³) | | | | | |
|---------------|--|--------|-------|------|----------------------|--------------------------|
| | E_{25} | h | N_c | k | $\Delta =$ $25.k$ | $E_c = K.$ E_Δ |
| Mean | 976.18 | 121.25 | 5.00 | 0.83 | 20.65 | 758.88 |
| SD | 174.51 | 5.17 | 1.22 | 0.04 | 0.89 | 147.15 |
| CV (%) | 17.88 | 4.26 | 24.49 | 4.31 | 4.31 | 19.39 |
| N | 5 | 5 | 5 | 5 | 5 | 5 |
| max | 1176.07 | 126.28 | 7.00 | 0.87 | 21.70 | 978.13 |
| min | 707.44 | 115.22 | 4.00 | 0.79 | 19.80 | 578.39 |

608 **Table 4:** Absorbed energy in 5.0 mm (E_5) in J, for cylinders of $\varnothing 150$ mm \times 150 mm and $\varnothing 100$ mm \times 100
 609 mm, according to the BCN test.

| Cylinders of $\varnothing 150$ mm \times 150 mm | | | | Cylinders of $\varnothing 100$ mm \times 100 mm | | | |
|--|--------------|--------------|--------------|--|--------------|--------------|--------------|
| C_f (kg/m ³) | 46.98 | 79.60 | 76.85 | C_f (kg/m ³) | 33.88 | 63.02 | 74.92 |
| Mean | 79.07 | 154.67 | 189.24 | Mean | 34.18 | 60.35 | 69.91 |
| SD | 17.61 | 26.64 | 39.81 | SD | 12.36 | 16.41 | 15.04 |
| CV (%) | 22.27 | 17.22 | 21.04 | CV (%) | 36.17 | 27.18 | 21.51 |
| N | 6 | 6 | 6 | N | 23 | 30 | 30 |
| max | 92.65 | 186.08 | 241.24 | max | 54.52 | 86.12 | 102.06 |
| min | 52.27 | 118.93 | 129.54 | min | 16.08 | 22.69 | 40.98 |

610

611 **Table 5:** Correlation for energy levels required by EN 14487-1 (2005) and BCN tests ($E_{Panel, 25}$ and $E_{BCN,}$
 612 $_{5.0, \delta}$ (mm)) in J, and average fibre content C_f in kg/m³.

| EN 14487-1 | EN 14488-5 | BCN (L) | BCN (S) | |
|-------------------|----------------------------|-----------------------------|-----------------------------|-------------------------|
| Class | E_{25} | $E_{5.0}$ | $E_{5.0}$ | C_f |
| E 500 | 500 (\pm 54) | 112 (\pm 19) | 50 (\pm 2) | 53 |
| E 700 | 700 (\pm 68) | 157 (\pm 15) | 70 (\pm 3) | 74 |
| E 1000 | 1000 (\pm 148) | 224 (\pm 36) | 100 (\pm 7) | 106 |

613

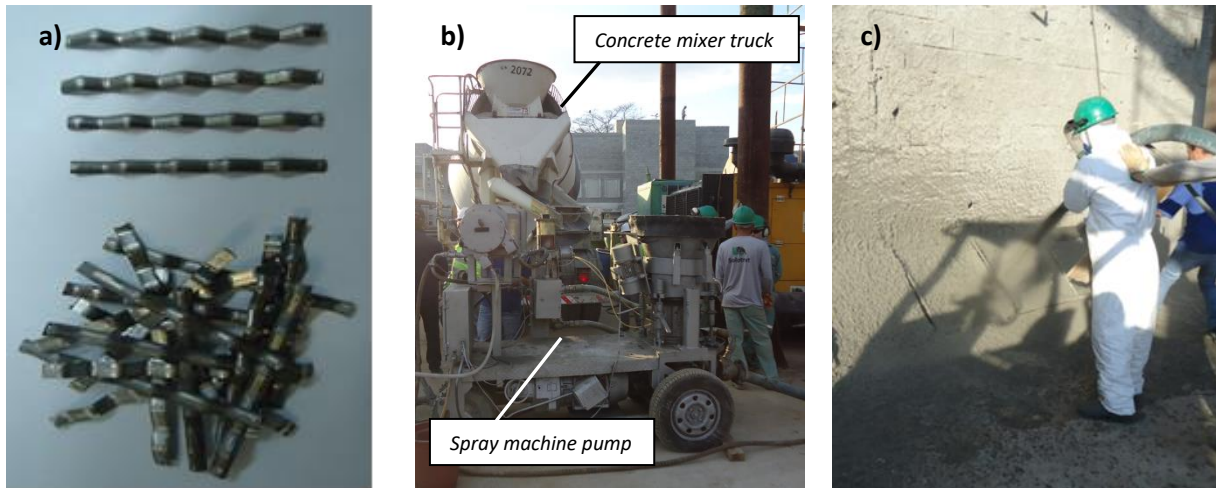
614 **Table 6:** Sample size (n) according to the statistical measurement values.

| 1 - α | 90% | 95% | 1 - α | 90% | 95% | 1 - α | 90% | 95% |
|--------------------------------|----------------|------------|--------------------------------|----------------|------------|--------------------------------|-------------------|------------|
| C_f (kg/m ³) | BCN (L) | | C_f (kg/m ³) | BCN (S) | | C_f (kg/m ³) | EN 14488-5 | |
| 46.98 | 6 | 9 | 33.88 | 10 | 15 | 33.88 | 1 | 2 |
| 79.60 | 4 | 5 | 63.02 | 6 | 8 | 63.02 | 1 | 2 |
| 76.85 | 5 | 8 | 74.92 | 4 | 5 | 74.92 | 5 | 8 |

615

616

617 **FIGURES**



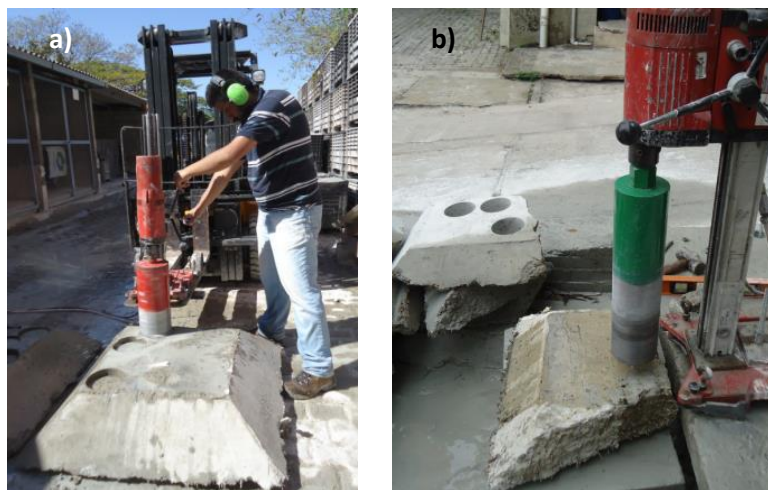
618
619 *Figure 1: Steel fibre used (a); concrete truck and pump (b); spraying process (c).*

620



621
622 *Figure 2: Square panel test according to EN 14488-5.*

623



624
625 *Figure 3: Cylinders extraction from large panels (a) and small panels (b).*

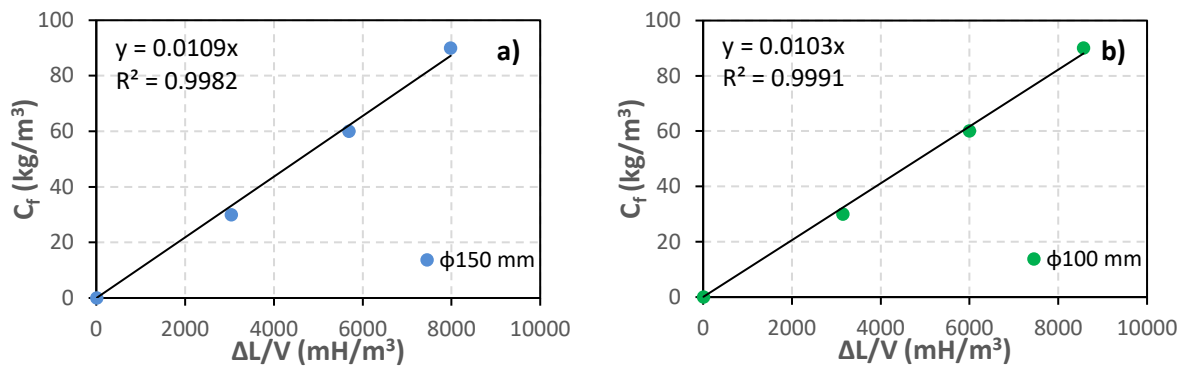
626



627 **Figure 4:** Barcelona test (BCN).

627

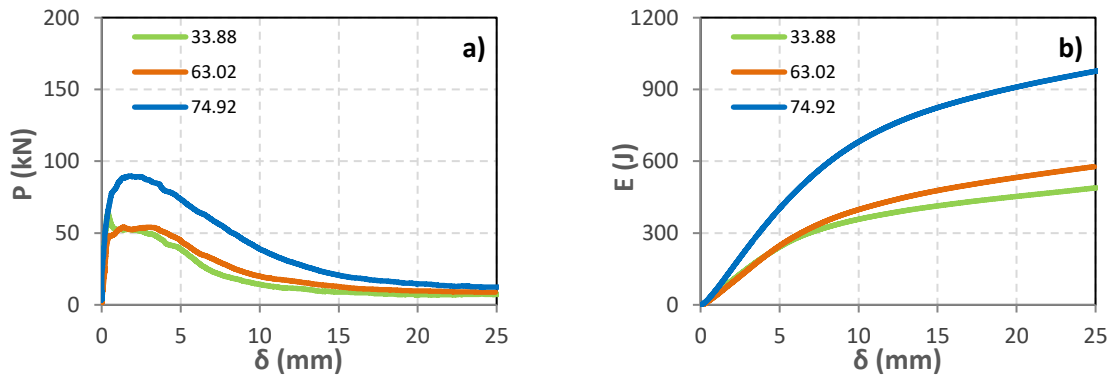
628



629

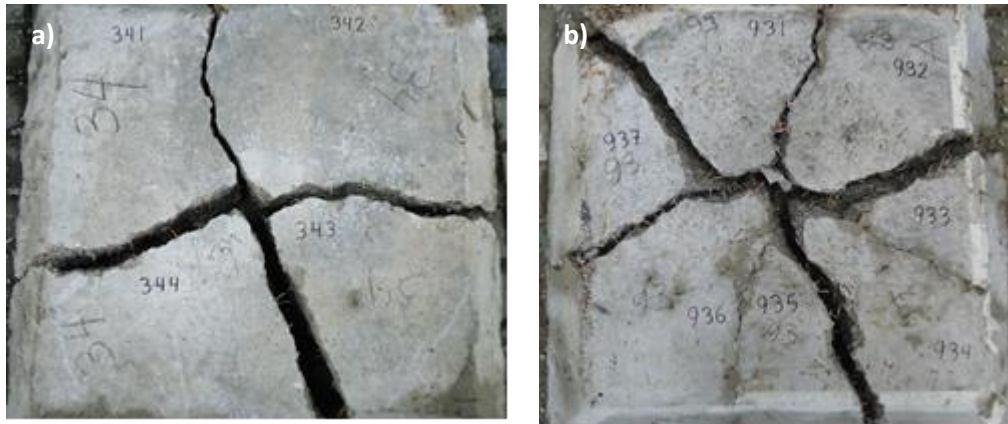
630 **Figure 5:** Inductive method calibration in styrofoam cylinders of $\text{Ø}150 \text{ mm} \times 150 \text{ mm}$ (a) and $\text{Ø}100 \text{ mm} \times$
631 100 mm (b).

632



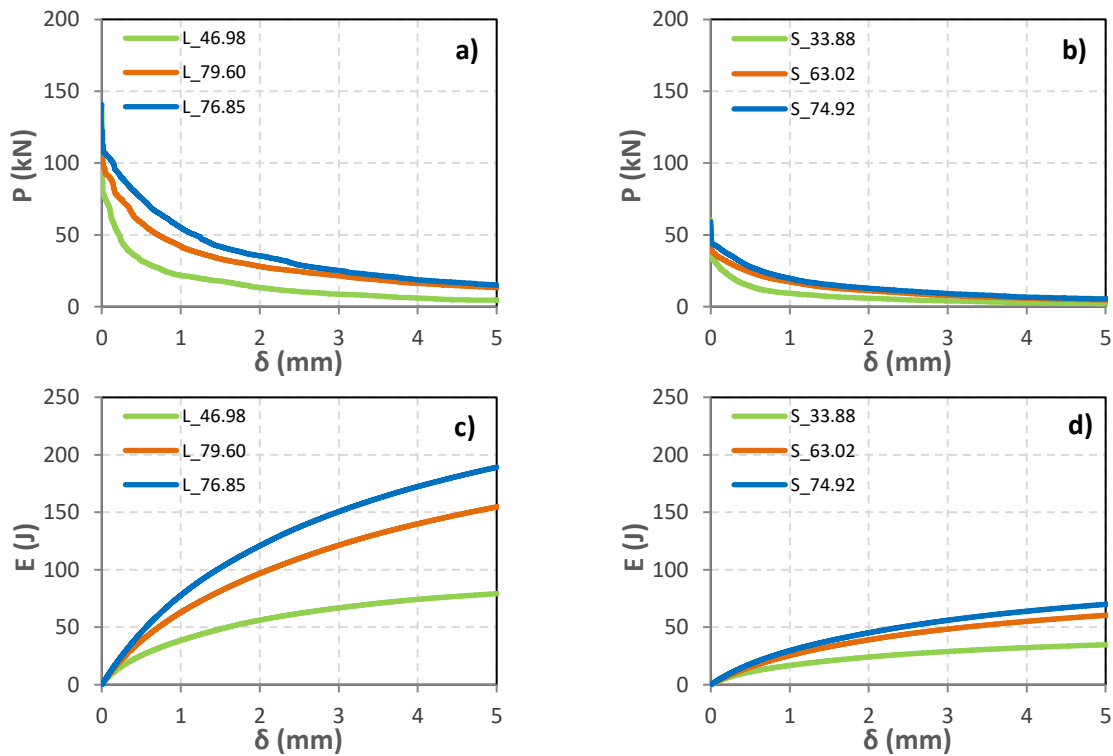
634 **Figure 6:** Average curves of load (a) and energy absorption (b) versus displacement, according to the EN
14488-5 test on small panels with fibre contents of 33.88, 63.02 and 74.92 kg/m^3 .

635



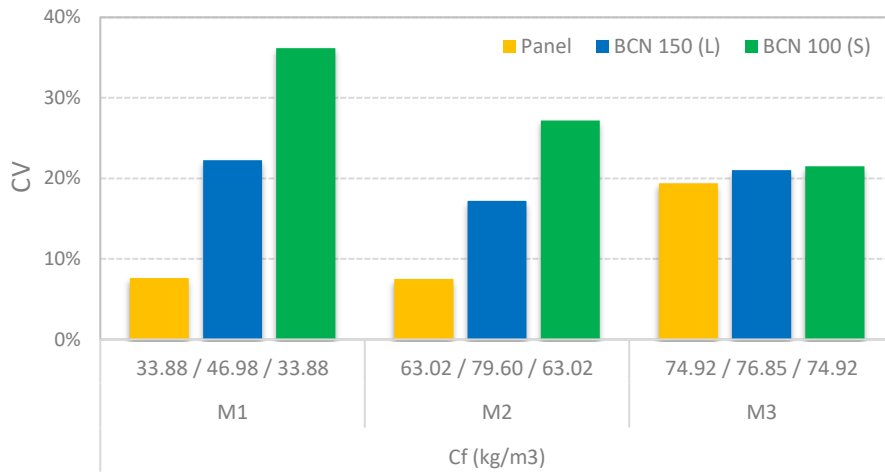
636
 637 **Figure 7:** Typical crack pattern including 4 major cracks for medium and lower fibre contents (a). Multiple
 638 cracks observed in panel with highest energy absorption for higher fibre contents (b).

639



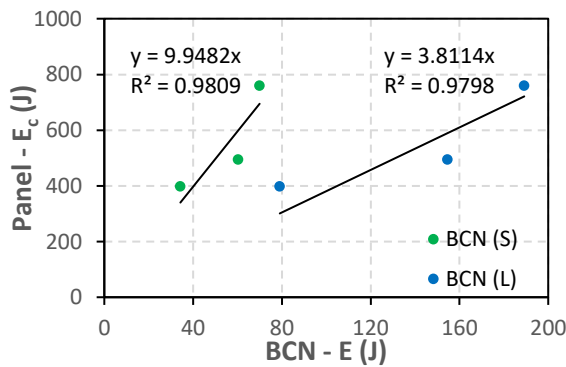
640 **Figure 8:** Average curves of load by displacement in cylinders of $\varnothing 150 \text{ mm} \times 150 \text{ mm}$ (fibre contents of
 641 $46.98, 79.60$ and 76.85 kg/m^3) (a) and $\varnothing 100 \text{ mm} \times 100 \text{ mm}$ (fibre contents of $33.88, 63.02$ and 74.92 kg/m^3)
 642 (b); and of energy absorption by displacement in cylinders of $\varnothing 150 \text{ mm} \times 150 \text{ mm}$ (c) and $\varnothing 100 \text{ mm} \times 100$
 643 mm (d) by the BCN test.

644



645
646
647
648

Figure 9: Comparison of the CVs of the energy absorption results of the EN 14488-5 test and BCN tests.



649

Figure 10: Correlation of average energy absorption results between the square panel test EN 14488-5 and BCN tests.

652

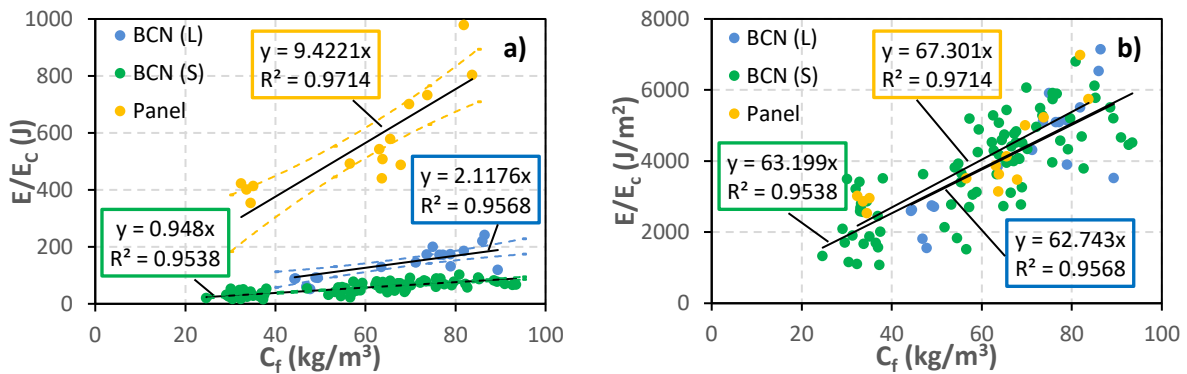


Figure 11: Correlation between energy absorption results from the square panel test EN 14488-5 and BCN tests with fibre content, in $J - kg/m^3$ (a) and $J/m^2 - kg/m^3$ (b).

655

656 **FIGURE CAPTION LIST**

657 **Figure 1:** Steel fibre used (a); concrete truck and pump (b); spraying process (c).

658 **Figure 2:** Square panel test according to EN 14488-5.

659 **Figure 3:** Cylinders extraction from large panels (a) and small panels (b).

660 **Figure 4:** Barcelona test (BCN).

661 **Figure 5:** Inductive method calibration in styrofoam cylinders of $\text{Ø}150 \text{ mm} \times 150 \text{ mm}$ (a) and
662 $\text{Ø}100 \text{ mm} \times 100 \text{ mm}$ (b).

663 **Figure 6:** Average curves of load (a) and energy absorption (b) versus displacement, according to
664 the EN 14488-5 test on small panels with fibre contents of 33.88, 63.02 and 74.92 kg/m^3 .

665 **Figure 7:** Typical crack pattern including 4 major cracks for medium and lower fibre contents (a).
666 Multiple cracks observed in panel with highest energy absorption for higher fibre contents (b).

667 **Figure 8:** Average curves of load by displacement in cylinders of $\text{Ø}150 \text{ mm} \times 150 \text{ mm}$ (fibre
668 contents of 46.98, 79.60 and 76.85 kg/m^3) (a) and $\text{Ø}100 \text{ mm} \times 100 \text{ mm}$ (fibre contents of 33.88,
669 63.02 and 74.92 kg/m^3) (b); and of energy absorption by displacement in cylinders of $\text{Ø}150 \text{ mm} \times$
670 150 mm (c) and $\text{Ø}100 \text{ mm} \times 100 \text{ mm}$ (d) by the BCN test.

671 **Figure 9:** Comparison of the CVs of the energy absorption results of the EN 14488-5 test and
672 BCN tests.

673 **Figure 10:** Correlation of average energy absorption results between the square panel test EN
674 14488-5 and BCN tests.

675 **Figure 11:** Correlation between energy absorption results from the square panel test EN 14488-5
676 and BCN tests with fibre content, in $\text{J} - \text{kg/m}^3$ (a) and $\text{J/m}^2 - \text{kg/m}^3$ (b).

677